Available online at www.sciencedirect.com

SCIENCE DIRECT®

Marine Micropaleontology 52 (2004) 217–240

MARINE MICROPALEONTOLOGY

www.elsevier.com/locate/marmicro

Abnormal carbonate diagenesis in Holocene–late Pleistocene sapropel-associated sediments from the Eastern Mediterranean; evidence from *Emiliania huxleyi* coccolith morphology

Daniela Crudeli[a,b,*], Jeremy R. Young[c], Elisabetta Erba[a], Gert J. de Lange[d], Karen Henriksen[e], Hanno Kinkel[b], Caroline P. Slomp[d], Patrizia Ziveri[f]

[a] *Department of Earth Sciences, University of Milan, Via Mangiagalli 34, 20133 Milan, Italy*
[b] *Institute for Geosciences, Christian-Albrechts-Universität Kiel, Ludewig-Meyn-str. 10, 24118 Kiel, Germany*
[c] *Palaeontology Dept., Cromwell Road, The Natural History Museum, London SW7 5BD, UK*
[d] *Department of Geochemistry, Faculty of Earth Sciences, Budapestlaan 4, 3584 CD Utrecht, The Netherlands*
[e] *Geological Institute, University of Copenhagen, Øster Voldgade, 10, 1350 Copenhagen C, Denmark*
[f] *Department of Paleoecology and Paleoclimatology, Faculty of Earth and Life Sciences, De Boelelaan 1085, 1081HV Amsterdam, The Netherlands*

Received 4 February 2003; accepted 23 April 2004

Abstract

In studying the Holocene–late Pleistocene record of the Eastern Mediterranean, considerable *Emiliania huxleyi* size/shape variation not clearly assignable to primary or secondary calcification was observed. Accordingly, different morphotypes were distinguished by light microscope (LM).

A subsequent scanning electron microscope (SEM) analysis of selected samples has indicated that *Emiliania huxleyi* coccoliths are variably affected by carbonate diagenesis in these sediments. A series of diagenetic stages were qualitatively defined, comprising well-preserved specimens, three overgrowth (OG1 to OG3) and one etching (E1) stage. Comparing SEM and LM observations, a tentative correlation between the *E. huxleyi* calcified LM-morphotypes and *E. huxleyi* SEM-overgrowth stages is proposed here.

Our study not only indicates that *Emiliania huxleyi* coccoliths are strongly influenced by carbonate diagenesis, but also that they show effects of carbonate precipitation and dissolution much more clearly than other coccoliths. The relative abundances of the different LM-morphotypes were used to define an *E. huxleyi* overgrowth index (EXO) that qualitatively estimates carbonate precipitation/dissolution on coccoliths in this sediment. This resulted in definition of five "Diagenetic" intervals (D1 to D5). Deposition of sapropel S1 was a time of good preservation with variable dissolution and no overgrowth of *E. huxleyi* coccoliths, whereas calcite overgrowth was high during the Last Glacial Maximum (LGM) and interglacial period and, to a lesser extent, during the Younger Dryas and through the last 5 ka.

Keywords: diagenesis; Mediterranean; *Emiliania huxleyi*; Holocene–late Pleistocene; sapropel S1

* Corresponding author. Present address: Institute for Geosciences, Christian-Albrechts-Universität Kiel, Ludewig-Meyn-str. 10, 24118 Kiel, Germany. Fax: +49-431-880-5557.

E-mail address: dc@gpi.uni-kiel.de (D. Crudeli).

0377-8398/$ - see front matter © 2004 Elsevier B.V. All rights reserved.
doi:10.1016/j.marmicro.2004.04.010

1. Introduction

A unique feature of late Neogene and Holocene sedimentation in the Eastern Mediterranean is the presence of rhythmic sapropel intervals, apparently recording basin-wide dysoxia. These sapropels, interbedded in pelagic–hemipalagic sediments, are rich in organic carbon (C_{org}> ~ 2 wt.%), characterised by a variable content of other elements and minerals (e.g. Fe, S, trace metals, kaolinite) and commonly have lower total carbonate content than their enclosing sediments (e.g. Calvert and Fontugne, 2001). The cyclicity of sapropel deposition is connected with precession-induced insolation maxima in the northern hemisphere (Rossignol-Strick et al., 1982; Rossignol-Strick, 1985; Hilgen, 1991; Lourens et al., 1996). Orbitally driven intervals of increased precipitation over parts of Africa and increased river run-off are thought to be the main environmental changes leading to sapropel formation (Rossignol-Strick et al., 1982; Rossignol-Strick, 1985; Freydier et al., 2001). Several studies, using different proxies, have been carried out over the past 25 years in order to understand the mechanisms by which the basin reacts to climatic change and induces sapropel formation, with debate mainly concentrated on the role of deep-water anoxia and/or enhanced productivity in producing organic carbon rich levels (see De Lange et al., 1999; Cramp and O'Sullivan, 1999; Thomson et al., 1999, for synthesis).

Several studies of calcareous nannofossils have been carried out in order to reconstruct the surface water dynamics during sapropel deposition (Violanti et al., 1991; Castradori, 1992, 1993a; Aksu et al., 1995a; Negri et al., 1999a,b; Negri and Villa, 2000; Negri and Giunta, 2001; Corselli et al., 2002; Giunta et al., 2003; Principato et al., 2003).

Selected works included detailed analyses of calcareous nannofossils assemblages within the youngest sapropel S1 (~ 6–9 ka, Mercone et al., 2000) (Violanti et al., 1991; Castradori, 1992, 1993a; Aksu et al., 1995a; Negri et al., 1999a; Negri and Giunta, 2001; Giunta et al., 2003; Principato et al., 2003). However, important aspects of the taxonomy applied to these assemblages have remained poorly defined, with key taxa being referred to informal groups or assigned to species which are usually confined to the Pliocene (Table 1). To resolve these problems we conducted a detailed light microscope (LM) and scanning electron microscope (SEM) study, with the objective of applying the taxonomy of modern coccolithophores to provide definitive identifications of all the common morphotypes. This paper is focused on the dominant species *Emiliania huxleyi* and associated reticulofenestrid coccoliths (Young, 1989) in order to: (a) quantify their distribution; (b) clarify their taxonomy; and (c) clarify the paleoceanographic and diagenetic history of Holocene–late Pleistocene sediments in the Eastern Mediterranean.

Our results indicate that most of the reported reticulofenestrid coccoliths are in fact *E. huxleyi* coccoliths affected by atypical early carbonate diagenesis, such forms are not observed from oceanic sediments which have undergone normal diagenesis.

1.1. Previous studies

In a core from south of Crete Violanti et al. (1991) recorded by LM small bridgeless reticulofenestrid coccoliths informally referred to "small" *Reticulofenestra* spp. and *Dictyococcites* spp. and noticed that these were particularly abundant above sapropel S1, between tephra Y-5 (35 ka, Keller et al., 1978) and the base of S1, but rare to absent within the sapropel, and very rare or absent below the tephra base. The authors discussed the possibility that the "anomalous assemblage" observed within the *Emiliania huxleyi* Acme Zone was reworked. Since such forms were systematically observed in numerous other cores from the same basin and at the same stratigraphic interval, Castradori (1992) discussed their taxonomy in more detail and, based on the work of Matsuoka and Okada (1989), tentatively referred them to *Reticulofenestra minuta*, *Reticulofenestra minutula* and *Dictyococcites productus,* a reticulofenestrid usually considered as confined to the Pliocene (e.g. Young, 1990, 1998). Following this, other authors have reported diverse reticulofenestrid communities from the Holocene–late Pleistocene of the Eastern Mediterranean, using variable informal nomenclature (Table 1; Fig. 1), and speculated on their palaeoecological significance. For example, Negri and Giunta (2001), observed a significant decrease of *Reticulofenestra*

Table 1
Presence of reticulofenestrids (Young, 1989) in the Eastern Mediterranean Holocene–late Pleistocene fossil record (#), surface sediment samples (##) and informal nomenclature applied to the assemblages

Authors	Type of sample	*E. huxleyi*	Small *Reticulofenestra* spp.	*Reticulofenestra* spp.	*Reticulofenestra* spp. (3–5 μm), (<3 μm)	Small *Reticulofenestra* (<3 μm)	*R. parvula* (3–5 μm)	*Reticulofenestra* "overcalcified" s.l.	*Dictyococcites* spp.	*Dictyococcites* sp.
Violanti et al., 1991	#	*	*						*	
Castradori, 1992	#	*	*						*	
Castradori, 1993b	#	*								
Negri et al., 1999a	#	*		*						
Negri and Giunta, 2001	#	*		*						
Giunta et al., 2003	#	*			*					*
Principato et al., 2003	#	*		*		*	*		*	
Ziveri et al., 2000a	##	*						*		

Negri et al. (1999a) report the presence of reticulofenestrids but do not show their record, Castradori (1993b) documents the *Emiliania huxleyi* pattern, details on reticulofenestrids are in Castradori (1992). The larger * indicates that the group includes the forms indicated by the smaller *.

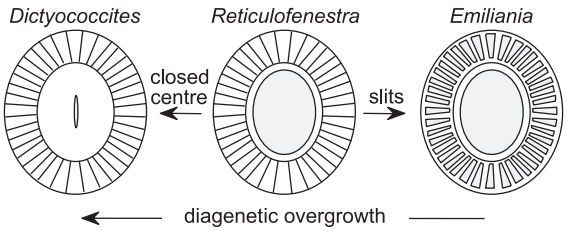

Fig. 1. Generic distinctions. The three genera *Reticulofenestra*, *Dictyococcites* and *Emiliania* have identical basic structure and differentiation of them is somewhat artificial. *Reticulofenestra* has the typical morphology, *Emiliania* is differentiated by presence of slits between elements, *Dictyococcites* by a closed central area (Young, 1989, 1998). These morphotypes are usually a product of primary variation, but in the material discussed here it seems likely that diagenesis has produced analogous variation from overgrowth of a single original species, *Emiliania huxleyi.* (N.B. *Gephyrocapsa* is also similar but has a bridge over the central area).

spp. within sapropel S1, and based on Negri and Villa (2000), who related this group to upwelling, suggested that this decrease was due to competition with siliceous plankton in the upper part of the photic zone. Principato et al. (2003) similarly interpreted the decrease in abundance of the reticulofenestrids within S1.

So, within the Eastern Mediterranean it has become conventional to interpret variable assemblages of reticulofenestrid coccolith morphotypes in terms of variable primary assemblages under ecological control. There are, however, problems with this interpretation. First, these variable assemblages are rarely recorded from other coeval sediments, even in the western Mediterranean (e.g. Flores et al., 1997; Sbaffi et al., 2001). Second, they are absent from modern assemblages, for example Ziveri et al. (2000a) reported from Eastern Mediterranean surface sediments, abundant *Reticulofenestra* "overcalcified" sp. coccoliths, but very few of these specimens were observed in deep water sediment trap samples. Moreover, it is noteworthy that, in the publications on the Holocene–late Pleistocene of the Eastern Mediterranean, *E. huxleyi* and the identified reticulofenestrids show roughly opposite trends in relative abundance with *E. huxleyi* decreasing both just below and above sapropel S1 (Violanti et al., 1991; Castradori, 1992, 1993b; Negri and Giunta, 2001; Principato et al., 2003).

1.2. Holocene–latest late Pleistocene reticulofenestrids

Emiliania huxleyi appeared in the late Pleistocene becoming a major component of the coccolith assemblages from the base of the *E. huxleyi* Acme Zone, quantitatively defined and dated at 85 ka by Rio et al. (1990), replacing *Gephyrocapsa* (Gartner, 1977; Thierstein et al., 1977; Rio et al., 1990; Raffi et al., 1993; Young, 1998). The dominance of *E. huxleyi* in the upper photic zone nannoflora of the Holocene and latest late Pleistocene is well documented both globally (e.g. Matsuoka and Okada, 1989; Rahman and de Vernal, 1994; Okada and Wells, 1997; Flores et al., 1999; Henriksson, 2000; Kinkel et al., 2000; Takahashi and Okada, 2000) and from the Mediterranean (Flores et al., 1997; Aksu et al., 1995a; Sbaffi et al., 2001).

Modern *Reticulofenestra* species are *Reticulofenestra parvula*, *Reticulofenestra punctata* and *Reticulofenestra sessilis* (Okada and McIntyre, 1977; Jordan and Kleijne, 1994) but *R. parvula* is the only species observed to date in Mediterranean water samples (Ziveri et al., 2000a; Cros, 2002) and surface sediments (Ziveri et al., 2000a). The species is rare to absent in Mediterranean surface waters (Cros, 2002 and Kleijne, 1993, respectively).

R. parvula has been reported to dominate in the upper part of marine isotope stage (MIS) 5 off of western Australia (Okada and Wells, 1997) and to be present in MIS2 (south Chatham Rise, southeastern New Zealand, Wells and Okada, 1997) but there are few other works reporting its fossil record, probably because the very small size of the placolith does not allow easy recognition by LM (Okada and Wells, 1997, and reference therein). Forms <2.5 μm with no bridge are usually grouped as small *Reticulofenestra* by LM (Takahashi and Okada, 2000).

The last occurrence of the common Neogene very small *Reticulofenestra* (<3 μm, Young et al., 1997) is not well established, however, small placoliths referable to *Reticulofenestra minutula* appear to go extinct close to the Plio-Pleistocene boundary possibly due to competition within the reticulofenestrids group (e.g. Young, 1998). Wells and Okada (1997) observed by SEM true *R. minutula* and discussed the possibility that these forms were reworked or that they persisted longer in the studied area.

Dictyococcites is used by some authors (e.g. Matsuoka and Okada, 1989; Rahman and de Vernal, 1994) but there is no consensus on the validity of this genus and specimens are thought to be *Reticulofenestra* ecophenotypes or *Reticulofenestra* specimens affected by diagenesis (Young, 1990, 1998).

1.3. Comparative studies of coccolith diagenesis

Pioneering work on coccolith diagenesis was performed by Roth and Thierstein (1972) and Roth (1973, 1978) who evaluated the state of preservation of samples from DSDP cores, and defined preservation categories based on the progressive disappearance of less solution-resistant species. The categories have been successfully applied to the oceanic fossil record (e.g. Roth, 1983; Raffi and Flores, 1995; Su et al., 2000). Very commonly in ancient oceanic sediments dissolution and overgrowth have been observed in the same sample and to be species preferential-related to the structure of the coccolith. Small coccoliths and delicate parts of coccoliths such as central cross structures and grills are easily dissolved and they are often absent even at early stages of diagenesis (Roth and Thierstein, 1972; Roth, 1973, 1978; Thierstein, 1980). By contrast, larger coccoliths and discoasters are more frequently preserved and often preferentially overgrown (e.g. Ramsay, 1972).

Winter (1982a,b) recorded *Emiliania huxleyi* coccoliths heavily affected by secondary calcite overgrowth and/or etching in upper Quaternary sediments from the Red Sea and discussed the possibility of taxonomic misidentification of overgrown forms observed, in the same basin, by McIntyre (1969) and Müller (1976).

2. Materials and methods

Eleven cores recovered from the Mediterranean basin between 339 and 3390 m water depth (Fig. 2; Table 2) aligned along E–W and N–S transects, were analysed as part of the Sapropels And Paleoceanography (SAP) project and a multidisciplinary investigation was carried out on samples from these cores. All cores from the Eastern Mediterranean recovered the Holocene sapropel S1, whereas cores from the Aegean Sea and Western Mediterranean contained no visual S1. The thickness of visual S1 and oxidised S1 (Van Santvoort et al., 1996; Thomson et al., 1999) (Figs. 3a–i) has been established by accurate comparison of Ba/Al, Mn, organic carbon and pyrite sediment profiles (De Lange et al., in prep.).

2.1. Tephra layers

The depth and thickness of tephra layers recorded in selected cores were traced on the basis of sedimentological description of cores and qualitative observation of glass fragments in the >150 and 63–150 μm fractions (Principato, 2003; Principato, pers. comm., 2000). In core SL60 concentration of

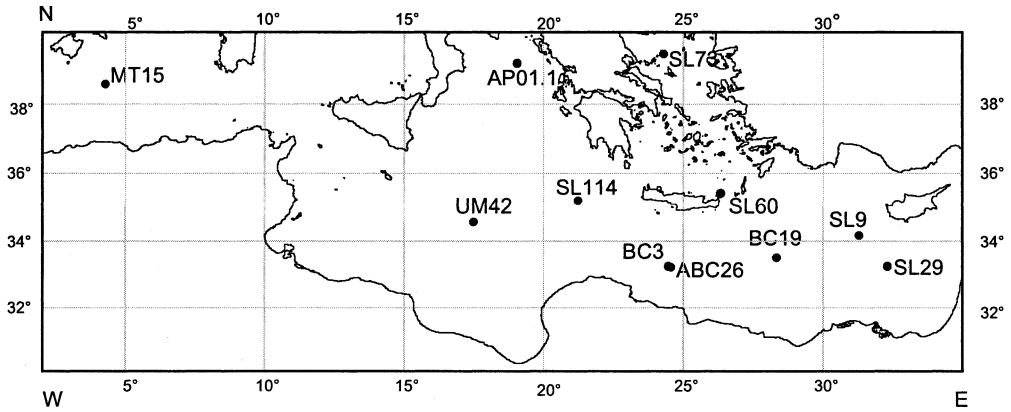

Fig. 2. Map of the Mediterranean Sea indicating the location of studied cores. Precise positions and depths are given in Table 2.

Table 2
Details of studied cores, number of analyzed samples and sampling resolution

Core name	Type	Cruise	Position	Depth (m)	Length (cm)	No. of samples	Resolution (cm)
MT15, sec.10-9	GC	Tyro 1993	38°53.75′ N–04°30.60′ E	2373	141	71	2
UM42	BC	Urania 18, 1994	34°57.23′ N–17°51.75′ E	1375	35	35	1
AP01.1, sec.1	GC	Urania 1998	39°12.99′ N–19°06.78′ E	811	80	53	1
SL114	BC	Logachev 1999	35°17.24′ N–21°24.52′ E	3390	49.5	48	1
SL73	BC	Logachev 1999	39°39.67′ N–24°30.65′ E	339	38.9	37	1
BC3	BC	Marion Dufresne 81, 1994	33°22.51′ N–24°46.00′ E	2180	86	59	1.2
ABC26	BC	Tyro 1987 leg 87/3	33°21.3′ N–24°55.70′ E	2150	27.4	44	0.6
SL60, sec.5, 6, 7	PC	Logachev 1999	35°39.69′ N–26°34.99′ E	1522	210	103	2
BC19	BC	Marion Dufresne 69, 1991	33°47.85′ N–28°36.50′ E	2750	35	34	1
SL9	BC	Logachev 1999	34°17.17′ N–31°31.36′ E	2302	45.2	44	1
SL29	BC	Logachev 1999	33°23.35′ N–32°30.18′ E	1587	39.5	38	1

The cores are stored at the Department of Geochemistry, Utrecht, the Netherlands.

glass fragments is estimated only on the base of smear slide observations.

During our smear slide analyses (cross-polarised light microscopy, 1250 ×), the presence of fine glass fragments (FGF) was semi-quantitatively estimated and reported as absent (N, null), scarce (S: 1–10 FGF/10 field of view (FOV)), common (C: >10 FGF/10 FOV), abundant (A: 1–5 FGF/1 FOV) or very abundant (VA: >5 FGF/1 FOV). Two tephra layers (Figs. 3a,c) were identified by glass fragments composition by L. Vezzoli (Insubria University). These methods are described by Principato (2003).

2.2. Light microscopy (LM)

The relative abundance of coccoliths was quantified by cross-polarised light microscopy (LM), using a Wild Leitz microscope, at 1250 × magnification. In total 566 samples were studied at an average sampling resolution of 1.5 cm (Table 2). Rippled smear slides were prepared, covered with a coverslip and permanently mounted with Norland Optical Adhesive. For each smear-slide three to four hundred coccoliths were counted, with an additional count of minor and lower photic zone species, following the concepts of Matsuoka and Okada (1989) and Castradori (1992, 1993a).

For the taxonomic study, the different *Emiliania huxleyi* morphotypes were observed and photographed by LM, using a Zeiss Axioplan microscope (1600 ×) connected to a CCD (Charged Couple Device) camera for image capture (Young et al., 1996) (Table 3). Sample EE0146 from core BC3 (0.8 cm from the top core) was chosen for detailed LM–SEM comparison of *E. huxleyi* coccoliths, as described in this work and over 70 LM (1600 ×) images were taken from this sample.

2.3. Scanning electron microscopy (SEM)

Selected samples below, within and above sapropel S1 from cores BC3 and UM42 were qualitatively observed by high resolution scanning electron microscopy, using a Philips XL30, Field Emission SEM (Table 3). In total 229 images were taken, including some 70 high magnification (usually 20,000 ×) images of reticulofenestrids. Having observed overgrown coccoliths in samples at different depths from the top of cores, particular attention was paid to sample EE0146 at 0.8 cm from the top of core BC3 in order to verify if similar carbonate diagenesis affected coccoliths close to the sediment/water interface and 29 reticulofenestrid specimens were imaged from this

Fig. 3. (a–i) Relative abundance record of *Emiliania huxleyi* Lightly Calcified morphotype (EHLC), *E. huxleyi* Moderately Calcified morphotype (EHMC), "*Reticulofenestra* overcalcified s.l." (ROC) and "*Dictyococcites* s.l." (DY) in studied cores from the Eastern Mediterranean. The dark grey colour represents the dark part of S1 and the light grey the oxidised part of the sapropel. Tephra layers are indicated by grey colour (see text for tephra identification). In all cores, the vertical axis represents depth (cm) from the top of core. (m–n) Relative abundance record of EHLM and EHMC* (see text for explanation) of ROC (m) and of Gephyrocapsid (n). The *E. huxleyi* overgrowth index (EXO) is reported for each cores; note the very different scale of figures m–n. Solid thicker lines define "Diagenetic" intervals D1–5 (see discussion for explanation).

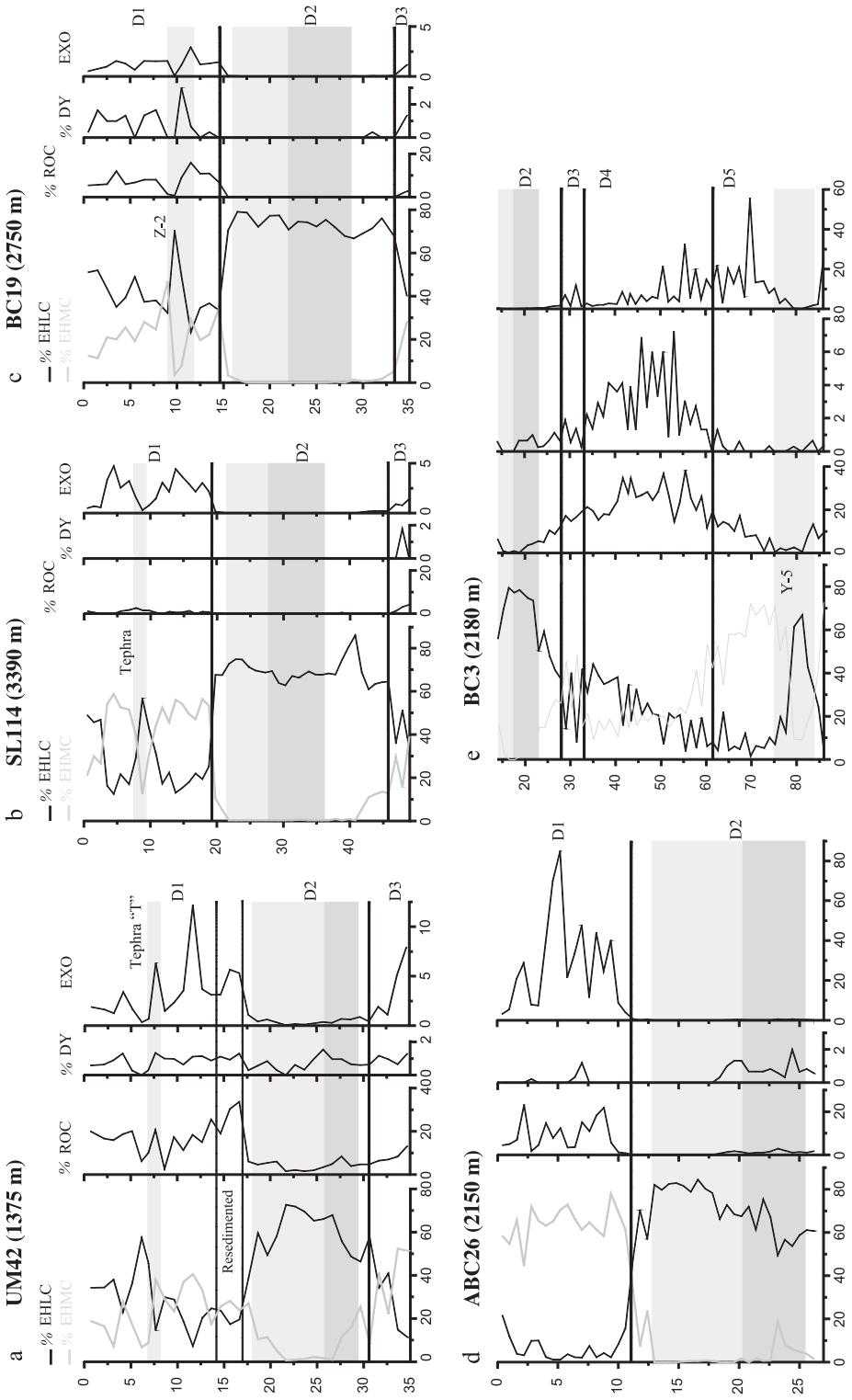
a UM42 (1375 m)
b SL114 (3390 m)
c BC19 (2750 m)
d ABC26 (2150 m)
e BC3 (2180 m)
% EHLC
% EHMC
% ROC
% DY
EXO
Tephra "T"
Resedimented
Tephra
Z-2
Y-5
D1
D2
D3
D4
D5

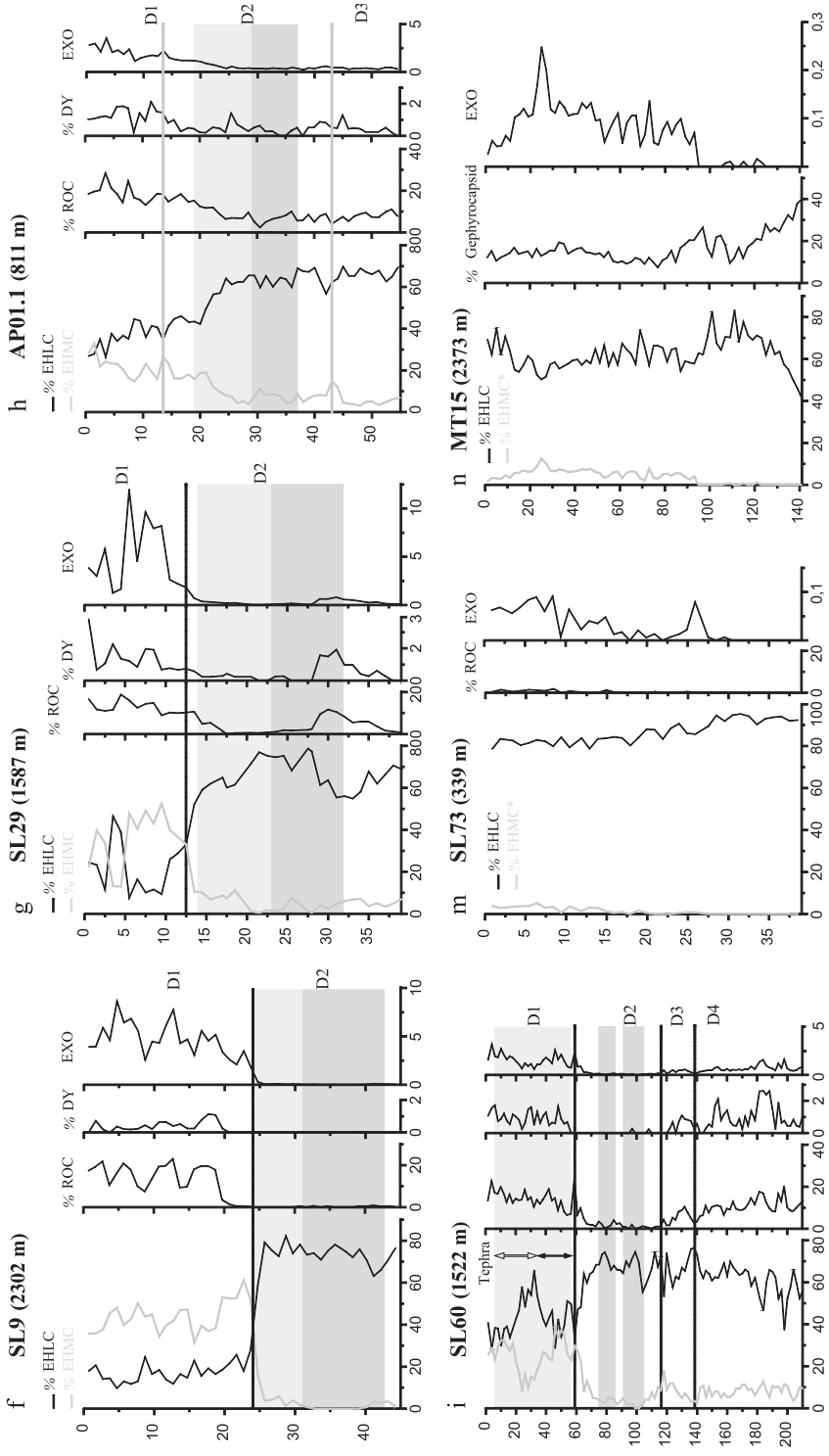

Fig. 3 (*continued*).

Table 3
Samples analysed by SEM and LM (1600 ×) and summary of SEM observations: *Emiliania huxleyi* coccolith normally preserved and at different diagenetic SEM-stages

Core	Sample code	Depth from top (cm)	*E. huxleyi*-normally preserved	*E. huxleyi*-E1	*E. huxleyi*-OG1	*E. huxleyi*-OG2	*E. huxleyi*-OG3	holococcoliths	OG-holococcoliths	small heterococcoliths	N. images (SEM)	N. images reticulofenestrids (SEM)	N. images reticulofenestrids (LM, 1600×)
BC3	EE0146	0.8	*	*	*	*		*	*	*	48	29	75
	EE0161	18.8	*	*	*		*	*		*	29	8	28
	EE0163	21.8		*				*		*	41	1	
	EE0167	26.6											60
	EE0168	27.8							*	*	5		
	EE0180	42.8			*	*	*			*	8	3	100
	EE0199	65				*	*			*		6	
	EE0203	69.8											60
	EE0213	83.6											51
UM42	DD01320	6.9	*		*						2	2	
	DD01344	18.65	*		*	*	*	*		*	19	5	
	DD01348	20.65			*			*	*	*	11	2	
	DD01352	22.65	*	*	*	*		*		*	23	12	
	DD01354	23.65									2		
	DD01356	24.65						*		*	7		
	DD01360	26.65	*					*			4	1	
	DD01362	27.65									2		
	DD01364	28.65						*			1		
	DD01366	29.65	*					*		*	12	1	
	DD01368	30.65						*		*	6		
	DD01376	34.65								*	3		

SEM observations on holococcoliths and other small heterococcoliths are also included. The dark grey colour represents the dark part of S1 and the light grey the oxidised part of the sapropel.

sample. Filter preparation for SEM study was based on the method of Andruleit (1996).

3. Results

In all the cores analysed, by LM, in addition to the *Emiliania huxleyi* morphotypes described below, *Gephyrocapsa* specimens have been observed. In this work their relative abundance is documented only in the Western Mediterranean core (Fig. 3n). *Gephyrocapsa* has a maximum abundance of 10% in core UM42, in other cores the abundance is usually < 5%. Cretaceous to Neogene calcareous nannofossils have been variably recorded by LM in all the cores, however, a systematic increase within the sapropel was not observed.

3.1. LM morphotype discrimination

In cores from the Eastern Mediterranean two morphotypes of *Emiliania huxleyi* coccoliths were distinguished under LM and separately quantified: *E. huxleyi* Lightly Calcified (EHLC) (Plate I, figures 1–3) and *E. huxleyi* Moderately Calcified (EHMC) (Plate I, figures 4–9). Two other morphotypes, not clearly referable to living species, were quantified and initially named "*Reticulofenestra* overcalcified s.l." (ROC) (Plate I, figures 10–12) and "*Dictyococcites* s.l." (DY) (Plate I, figures 13–15), respectively.

Distinction between EHLC and EHMC was based on the appearance of the outline, size of the central area opening and coccolith brightness (compare Plate I, figures 1–3 with figures 4–9). The distinction between EHMC and ROC was primarily based on observation of the outline, which is well defined and serrated in ROC. In addition, ROC specimens are brighter and larger than EHMC specimens (compare Plate I, figures 4–9 with figures 10–12). Central area length and width show a broadly similar range of values in the two morphotypes. DY was distinguished from ROC by its higher brightness and completely closed central area. The majority of coccoliths identifiable as ROC or DY are larger than EHMC but there is considerable overlap in their size ranges.

The characters used for LM discrimination are summarised in Table 4; size variability observations are based on systematic observations of morphotypes from some 500 samples.

In cores SL73 from the Aegean Sea and MT15 from the Western Mediterranean, while the EHLC morphotype was clearly present, the EHMC morphotype was not observed. Here, in addition to EHLC and extremely rare coccoliths assignable to ROC and DY by LM, coccoliths showing a higher brightness were observed and separately counted as EHMC*. These forms very rarely show a closed central area.

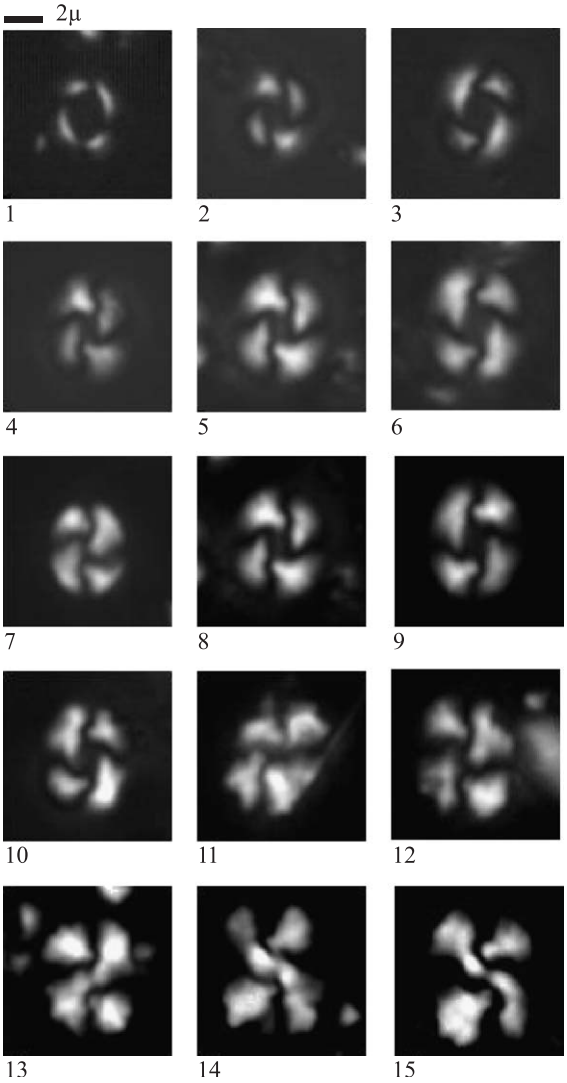

Plate I. Figures 1–15. Cross polarised light images of *Emiliania huxleyi* morphotypes; all specimens from core BC3, 0.8 cm except figure 1 from core BC3, 18.8 cm within S1. Figures 1–3. *E. huxleyi* Lightly Calcified morphotype (EHLC). Figures 4–9. *E. huxleyi* Moderately Calcified morphotype (EHMC). Figures 10–12. "*Reticulofenestra* overcalcified s.l." (ROC). Figures 13–15. "*Dictyococcites* s.l." (DY).

3.2. LM quantitative analyses

3.2.1. Eastern Mediterranean cores

3.2.1.1. Sedimentary interval below sapropel S1. In core BC3 EHLC and EHMC show close-spaced fluctuations with a general opposite trend in relative abundance (Fig. 3e). In detail EHLC abruptly increases in relative abundance from the core bottom and shows two peaks (>60%) within tephra Y-5. A decrease of EHMC below S1 is detected in this last core BC3 as in others (Figs. 3a–c). Here the morphotype is mostly replaced by EHLC. In cores AP01.1 and SL60 EHLC dominates and EHMC, commonly, has average values <10% (Figs. 3h–i). In the other cores EHMC is scarce to absent (Fig. 3g and figs. 3d,f, respectively). In core BC3, ROC and DY have relative abundance values >20% and >2%, respectively, at the middle part of the core and decrease upwards (Fig. 3e). The morphotypes have average values of about 10% and 1% in selected cores (Figs. 3a,h–i) but are scarce to absent in other (Figs. 3b–d,f–g).

3.2.1.2. Sapropel S1. EHLC is the dominant morphotype within the sapropel in all the cores (Figs. 3a–i). Calcified morphotypes, EHMC, ROC and DY are variably present in some cores (Figs. 3a,d–e,g–i) but are rare to absent in others (Figs. 3b–c,f). Noteworthy, in selected cores, is the increase of EHMC in the upper part of the oxidised sapropel (Figs. 3a,e–h). EHMC and ROC slightly increase in correspondence of S1 interruption in core SL60, where a minor decrease of EHLC is observed (Fig. 3i).

3.2.1.3. Sedimentary interval above sapropel S1. In most cores, a remarkable change in dominance between the four LM morphotypes occurs in the interval above S1. EHMC is very common and, in most cores, abruptly becomes even more abundant than EHLC. In detail, EHLC shows continuously higher percentage values than EHMC only in core AP01.1 and SL60 (Figs. 3h–i). High percentage values of ROC (32%) just above S1 have been detected in core UM42 (Fig. 3a) within an interval characterized by redepositional processes (E. Schefuß, pers. com.; Principato, 2003).

3.2.2. LM morphotypes in tephra layers

Potentially interesting trends in LM morphotypes were observed in short intervals containing tephra layers. The ash layer recovered in core UM42, termed tephra "T" (L. Vezzoli, pers. comm., 2000) (Fig. 3a),

Table 4
LM characters observed in qualitatively identifying the *Emiliania huxleyi* LM morphotypes from the Eastern Mediterranean cores during counting, coccoliths maximum dimension and range of variability of the central area (CA)

LM characters	EHLC	EHMC	ROC	DY
Appearance of outline	defined	less defined	serrate	serrate
Appearance of the CA	open	closer	closer	closed
Brightness	low/normal	higher	higher	higher
Outline	narrowly elliptical	normally elliptical	narrowly to broadly elliptical	narrowly to broadly elliptical
Coccolith size	very small–small	small–medium	small–medium	small–medium
Coccolith length (μm)	2–4.5	3–5.5	3.5–7	3.5–7
Coccolith width (μm)	1.5–3	2.5–4	2.5–4.5	2.5–4.5
CA length range (μm)	1.5–3	1.5–2.5	1–2.5	–
CA width range (μm)	1–2	1–1.5	0.5–1.5	–
LM–SEM correspondance	EHLC = normal–E1–OG1	EHMC = OG1–OG2	ROC = OG2–OG3	DY = OG3

For subdivision of *Emiliania huxleyi* morphotypes in cores SL73 and MT15, see text explanation. Last row, suggested correspondence between LM–SEM morphotypes.

has been related to a basaltic Plinian Etna eruption that occurred at 122 years BC (Coltelli et al., 1998). The tephra in core BC3 identified as Y-5 occurred at 35 ka BP (Keller et al., 1978) (Fig. 3e), whereas the tephra recovered in core BC19 has been identified as Z-2 (Fig. 3c), correlated with the 1359 ± 17 years BC (Narcisi and Vezzoli, 1999) Santorini eruption. Details of the Holocene tephra layers recorded in cores SL114 and SL60 (Figs. 3b,i) will be given in a separate publication.

EHLC shows remarkable peaks in relative abundance at tephra with average values of 60% (Figs. 3b–c,e) except in core UM42 in which a clear shift of EHLC has been observed just above the tephra (Fig. 3a). In core SL60 EHLC abruptly increases in relative abundance at the base of tephra and shows oscillations opposite to EHMC upwards (Fig. 3i).

3.2.3. Aegean Sea and Western Mediterranean

Two co-eval cores studied from outside the Eastern Mediterranean show quite different patterns in LM morphotypes. EHLC dominates with average relative abundance of 85% throughout the Aegean Sea core, whereas EHMC* has average percentage < 5% and the other morphotypes are extremely rare and are not plotted (Fig. 3m).

In the Western Mediterranean core EHLC dominates being replaced by the Gephyrocapsid group (mainly small *Gephyrocapsa* and *Gephyrocapsa oceanica*) at the lower part of the core, whereas EHMC* has been observed in the upper part of the core and shows relative abundance < 13% (Fig. 3n). The other two morphotypes are present only in two samples with extremely low abundance.

3.3. SEM analyses

We observed strong diagenetic effects on *Emiliania huxleyi* coccoliths and even within a single sample there was variation from well-preserved *E. huxleyi* coccoliths to massively overgrown specimens (Table 3, Plate II). To document this, 67 specimens were photographed and then subjectively classified into three overgrowth stages, OG1–OG2–OG3, normal preservation, and one dissolution stage, E1. Careful examination of these specimens revealed that the variation was continuous, with a complete sequence of intermediates occurring between the best preserved coccoliths and those which required considerable care even to identify.

Gephyrocapsa specimens were rarely observed and detailed observations were not made for these specimens. Reworked calcareous nannofossils and *Reticulofenestra* specimens were not observed during SEM analyses.

Coccoliths of *E. huxleyi* not affected by overgrowth can be assigned to type A (Young and Westbroek, 1991) and are normally formed (Plate II, figures 1–3). Type B and C coccoliths (Young and Westbroek, 1991), *E. huxleyi* var. *corona* (Okada and McIntyre, 1977) and forms with variable non-genotypic calcification of the central area, as documented

by Young and Westbroek (1991), Cros (2002) and Beaufort and Heussner (2001), were not observed, although the presence of strongly modified specimens precludes certain identification of some coccoliths.

At stage OG1 and progressively through stage OG2, calcite overgrowth occurs syntactically on elements of the distal and proximal shields making them thicker, and longer by overgrowth upwards and outwards (Plate II, figures 7–12). Overgrowth also occurs on the tube elements, progressively closing the central area. At stage OG3 the elements of the coccolith are highly overgrown and distinction between proximal or distal shield and specific determination is difficult (Plate II, figures 13, 15). Slight dissolution of overgrown elements (Plate II, figure 8) as well as irregular crystal growth in the central area (Plate II, figures 7 and 10) has been observed.

Coccoliths with normal preservation, or affected by slight etching (E1), or slightly overgrown, often show dissolution of the distal shield elements (Plate II, figures, 4–6, 8, 13). At E1, the elements of the central area, are commonly partially dissolved (Plate II, figure 5) and preferential dissolution of the tube elements has been observed (Plate II, figures 4–5). Etched coccoliths have been more commonly observed in samples from sapropel S1, both the oxidised and dark part (Plate II, figures, 5, 6, 13). Mechanical breakage of coccoliths is also observed (Plate II, figure 6).

3.4. SEM–LM comparison

The SEM observations lead us to reinterpret our previous LM observations of these samples. In particular, From sample at 0.8 cm from the top of core BC3, specimens showing a range of preservation states/morphotypes are illustrated in Plate I (LM, figures 2–15) and Plate II (SEM, figures 1–2, 4, 8–9, 11–12). The different LM morphotypes are reinterpreted below and assigned to diagenetic stages. The suggested correspondence between SEM–LM morphotypes is summarised in Table 4.

3.4.1. EHLC=*Emiliania huxleyi* normal–*E. huxleyi* etched–*E. huxleyi* overgrowth stage OG1

In LM, EHLC (Table 4; Plate I, figures 1–3) is similar to the typical LM images of *Emiliania huxleyi* (e.g. Young et al., 1996). In particular, in sapropel S1 samples, forms referable to EHLC represented by thinner coccoliths (e.g. compare Plate I, figure 1 with figures 2–3) are more common. Nevertheless, during LM analyses any distinction and quantification would be subjective. This LM morphotype likely corresponds to both normally preserved and etched coccoliths (Plate II, figures 1–3 and figures 4–5, respectively).

By SEM, we have qualitatively observed the very common presence of OG1 coccoliths (Plate II, figures 7–9) in samples with low abundances of EHMC, ROC and DY. This suggests that OG1 coccoliths are also included in EHLC.

3.4.2. EHMC=*Emiliania huxleyi* overgrowth stages OG1–OG2

Coccoliths of the EHMC morphotype are small to medium in size, normally elliptical coccoliths (Table 4; Plate I, figures 4–9). Overgrowth stage OG1 and progression through OG2 initially results in a brighter image (Plate I, figures 4–9) related to the increased thickness of the coccolith (Plate II, figures 7–12).

Plate II. Figures 1–15. SEMs of *Emiliania huxleyi* coccoliths; variation in degree of primary calcification, secondary dissolution and secondary calcite overgrowth. Figure 1. Distal view of a normally preserved coccolith with moderate primary calcification (core BC3, 0.8 cm). Figure 2. Distal view of a normally preserved coccolith with high variation in primary calcification extending outward on the distal shield elements and affecting the tube width; central area elements affected by primary overgrowth (core BC3, 0.8 cm). Figure 3. Proximal view of a normally preserved coccolith partially broken with different spacing of the elements (core UM42, 22.65 cm). Figure 4. Distal view of a coccolith affected by etching (E1), central grill partially dissolved, dissolution affecting the T-shape termination of elements (core BC3, 18.8 cm). Figure 5. Distal view of a coccolith affected by etching (E1), proximal shield partially broken, central grill partially dissolved (core BC3, 18.8 cm). Figure 6. *Emiliania huxleyi* coccoliths affected by overgrowth, etching and mechanical breakage (core BC3, 18.8 cm). Figure 7. Distal shield of a coccolith at OG1 (core UM42, 22.65 cm). Figure 8. Distal shield of a coccolith at OG1, the elements are differentially affected by incipient dissolution (core BC3, 0.8 cm). Figure 9. View of the proximal shield of a coccolith at OG1 with preserved elements of the central area. On the left side fragments of holococcoliths (core BC3, 0.8 cm). Figure 10. Coccoliths at OG2 with irregular crystals growth at the central area (core UM42, 22.65 cm). Figure 11. Distal shield of a coccolith at OG2 (core BC3, 0.8 cm). Figure 12. Proximal shield of a coccolith at OG2 (core BC3, 0.8 cm). Figure 13. Distal shield of an *E. huxleyi*? coccolith at OG3. On the left side an *E. huxleyi* distal shield affecting by slight etching (E1) (core BC3, 18.8 cm). Figure 14. *Acanthoica quattrospina* and proximal view of *E. huxleyi* (core BC3, 18.8 cm). Figure 15. Proximal shield of a coccolith at OG1 (OG2?) (left side) and *Algirosphaera robusta* overgrowth (right side) (core BC3, 42.8 cm).

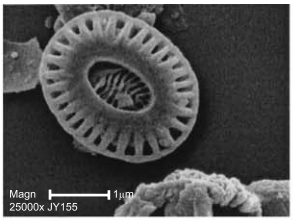

1

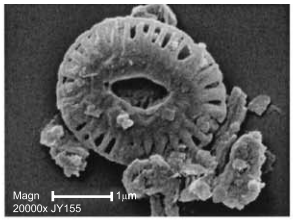

2

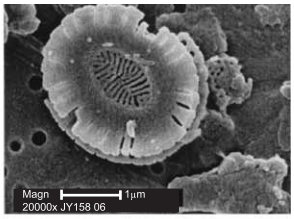

3

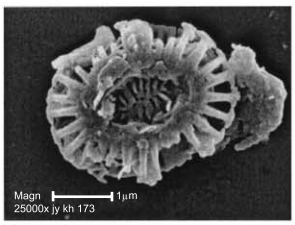

4

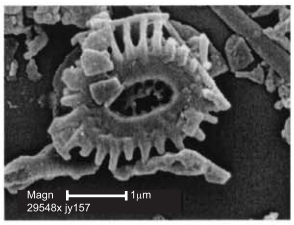

5

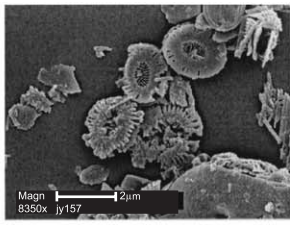

6

7

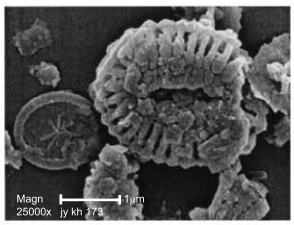

8

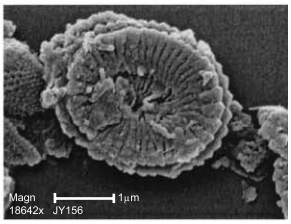

9

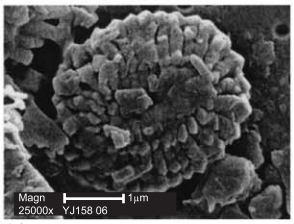

10

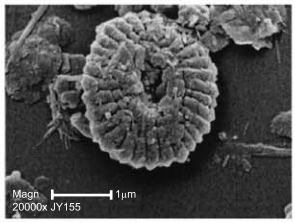

11

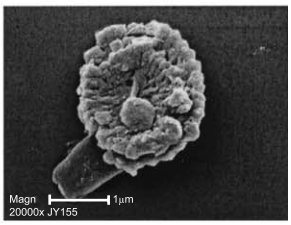

12

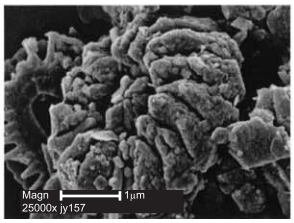

13

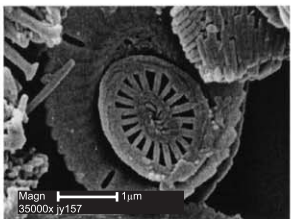

14

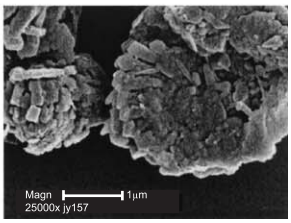

15

Usually, because shields of normal *Emiliania huxleyi* are thin, the rim edge is barely visible in cross-polarised light (Young et al., 1996). As overgrowth progresses, the crystals thicken and the rim of the coccolith becomes clearly visible in cross-polars. In addition, this secondary overgrowth produces an artificial increase in maximum dimensions of the coccoliths. The diffuse outline observed in EHMC (Table 4) can be related to the different thickness of crystal outgrowths. Moreover, on coccoliths of *E. huxleyi* at OG1–2 secondary calcification affects the tube elements (Plate II, figures 7–8, 11) resulting in a more closed central area in LM (Plate I, figures 7–9).

3.4.3. ROC=Emiliania huxleyi overgrowth OG2–OG3

In the advanced stages of overgrowth OG–2 and OG–3 most elements are heavily calcified and secondary calcite occurs in the central area (Plate II, figures 10–11, 13). This will result in a more serrated outline, higher birefringence, increase in maximum dimensions and a closed central area in LM, i.e morphotype ROC (Table 4; Plate I, figures 10–12).

3.4.4. DY=Emiliania huxleyi overgrowth OG 3

At SEM OG3 (Plate II, figures 13, 15) all elements of *Emiliania huxleyi* are widely affected by recrystallization and overgrowth completely closes the central area. This will give rise to DY type coccoliths in LM, with a brighter figure, high interference colour and completely closed central area (Plate I, figures 13–15).

4. Discussion

4.1. Diagenetic interpretation of LM morphotype variation

4.1.1. Eastern Mediterranean

The SEM–LM comparison of assemblages from selected samples, strongly indicated that the morphotype variation observed in LM was due to variable overgrowth of *Emiliania huxleyi* coccoliths and, for these samples, this required a re-interpretation of the morphotypes identified by LM as described above (Table 4).

From an equivalent time period, coccoliths identified as ROC and DY (Plate I, figures 10–15) are not reported from the Western Mediterranean (e.g. Flores et al., 1997) or oceanic sediments (e.g. Flores et al., 1999). This supports the inference that the forms seen in the Eastern Mediterranean (Figs. 3a–i) do not represent discrete, in situ, species. An alternative possibility which needs to be considered is that they represent reworked specimens.

Sapropels do usually contain reworked calcareous nannofossils, and these have been related to enhanced continental sediment input due to higher precipitation during sapropel deposition (Negri et al., 1999a; Corselli et al., 2002). Our LM study evidenced a variable presence of Cretaceous and Neogene calcareous nannofossils in sapropel S1 of some cores and the absence in others. However, the morphotypes ROC, DY and EHMC, which could include some reworked Neogene small reticulofenestrids, are preferentially present above and below S1 rather than within S1 (Figs. 3a–i) where reworked species have been predicted to occur (Negri et al., 1999a). Moreover, these calcified morphotypes are not systematically accompanied by other Neogene calcareous nannofossils (e.g. *Discoaster*). We cannot exclude the possibility that some reworked forms are included in the morphotypes discussed, but none of our observations supported this hypothesis. In particular, comparison with previous works (Violanti et al., 1991; Castradori, 1992, 1993b) indicates that the abundance of our morphotypes ROC and DY between tephra Y-5 and S1 base (Fig. 3e) is basinwide in the eastern basin which argues against reworking.

We did not observe *Reticulofenestra parvula* during SEM, however, we do not exclude that some of these forms are included in the EHLC LM group. Since *Gephyrocapsa* is commonly $<5\%$ (our unpublished LM data) in the cores analysed, we also assume that specimens that have lost or do not have the bridge do not influence substantially the pattern of EHLC.

Emiliania huxleyi does show significant variation in primary calcification (Young and Westbroek, 1991; Young, 1994) as well as variable non-genotypic calcification of the central area (Young and Westbroek, 1991; Cros, 2002; Beaufort and Heussner, 2001). In particular, from the Bay of Biscay Beaufort and Heussner (2001) observed *E. huxleyi* coccospheres characterised by different primary calcification of the central area and distinguished two morphotypes (their open and closed *E. huxleyi* morphotype). Their closed mor-

photype was dominant during summer and suggested a control of ecology on coccoliths morphology (Beaufort and Heussner, 2001). The possibility that EHLC and EHMC represent two different primary types and that their roughly opposite patterns (Figs. 3a–i) are due to a primary variation in *E. huxleyi* assemblages throughout time needs to be considered. Our EHLC could correspond to the open *E. huxleyi* morphotype observed by Beaufort and Heussner (2001) dominating during winter. However, EHLC, is more common in S1 formed during a warm period rather than outside the sapropel. EHMC, that could correspond to the closed *E. huxleyi* morphotype more common in summer (Beaufort and Heussner, 2001), decreases within the sapropel.

Whereas it is likely that the four LM-morphotypes identified in our study include coccoliths with variable primary calcification, the pattern of EHLC and EHMC in particular (Figs. 3a–i), do not reflect a primary variation in *Emiliania huxleyi* coccoliths assemblages.

4.1.2. Aegean Sea and Western Mediterranean

No samples were analysed by SEM from the Aegean Sea and Western Mediterranean but LM analyses were undertaken (Figs. 3m–n).

On the base of the comparison between the SEM–LM types from the eastern basin the rare ROC and DY could be assigned to OG2–3 forms. The possibility that some reworked small *Reticulofenestra* are included in these types is unlikely since definite reworked Neogene taxa (e.g. *Discoaster, Sphenolithus*) are very rare where ROC and DY are present.

EHLC probably includes both normally preserved and etched *E. huxleyi* coccoliths and bridgeless *Gephyrocapsa* specimens since both water and surface sediments samples are enriched in these forms (Knappertsbusch, 1993).

From the Western Mediterranean, Flores et al. (1997) and Colmenero-Hidalgo et al. (2002), observed dissolution of *E. huxleyi* rather than overgrowth and similar observations were made on surface sediments by Cros (2002). Moreover, informal groups similar to those reported from the Eastern Mediterranean (Table 1) have not been observed in studies of the Western Mediterranean (e.g. Flores et al., 1997). Given this it is possible that the EHMC* morphotype identified in our study reflects primary variation rather than overgrowth.

4.2. Are there Reticulofenestra coccoliths in the Holocene–late Pleistocene of the Eastern Mediterranean Sea?

We did not observe any *Reticulofenestra* specimens in our SEM study. This result is at odds with previous records from studies of Mediterranean Holocene–late Pleistocene sediments (Table 1), so we reviewed the available evidence to see if it is likely that previous records were based on misidentification of overgrown *Emiliania huxleyi* coccoliths.

In the Holocene–late Pleistocene, Violanti et al. (1991) and Castradori (1992) recorded, but did not illustrate, common small *Reticulofenestra* spp. and *Dictyococcites* sp. Based on their descriptions we believe these forms correspond to EHMC and to more heavily calcified coccoliths (i.e. ROC and DY), respectively. Negri and Giunta (2001) also recorded common *Reticulofenestra* sp., and illustrated them with LM and SEM images. Re-examination of their SEM images (their Plate I, figures 7 and 8) suggests they correspond to *E. huxleyi* OG2, whilst their LM images (their Plate I, figures 2–3) are similar to our EHMC. Ziveri et al. (2000a) reported *Reticulofenestra* overcalcified sp. from deep sediment trap and surface sediment samples. They illustrate two specimens: one (their Plate II, figure 7) is very similar to our *E. huxleyi* OG2 and a similar specimen is visible in an assemblage view (their Plate II, figure 10, form in the centre). The other specimen (their Plate II, figure 8) is similar to our *E. huxleyi* OG3 but this is more questionable due to extreme recrystallization. As already discussed, the possibility that the previous records are based on misidentification of overgrown *E. huxleyi* coccoliths is further supported by the general opposite trend of these forms and *E. huxleyi* (Violanti et al., 1991; Castradori, 1992, 1993b; Negri and Giunta, 2001; Principato et al., 2003).

We also suspect that reticulofenestrids recorded in the Holocene and late Pleistocene of the Aegean Sea and Black Sea as *Productellus doronicoides* (Aksu et al., 1995a,b), and *Reticulofenestra* spp. (Aksu et al., 2002) respectively, are in part overgrown coccoliths of *E. huxleyi* and/or of *Gephyrocapsa*. Our suspicions are based on the occurrence of these form in core-top sediments with an abundance trend opposite to that of *E. huxleyi* and to *Gephyrocapsa* species (Aksu et al., 1995b, their

Figs. 10 and 11) and to that of *E. huxleyi* (Aksu et al., 2002).

4.3. Preferential diagenesis of Emiliania huxleyi?

Ziveri et al. (2000a), observed a few overgrown specimens of *Emiliania huxleyi* in deep sediment trap samples (3000 m water depth) and more common specimens in core-top sediments with variable abundance at different sampling stations (their Fig. 4c). The rare overgrown forms observed in the water column could be resuspended specimens that have experienced diagenesis at the sediment/water interface. Sample at 0.8 cm from the top core (BC3) was extensively observed by SEM and clearly indicated the presence of a variable overgrowth assemblage as the other samples from the top of the cores contain a variable amount of calcified forms (Figs. 3a–i). Given the absence of strongly overgrown coccoliths in surface waters and their rarity in the water column, but common occurrence in surface sediment samples, we infer that the alteration mainly occurs at the sediment water interface and likely within the first millimetres–centimetres of sediments.

The amount of primary calcite incorporated in coccoliths of *E. huxleyi* is variable and commonly results in variation of thickness of the distal shield elements, proximal shield slitting and width of the inner tube (Young and Westbroek, 1991). In addition to these variations, inward growth of inner tube elements (Cros, 2002) and closure of the central area are likely ecologically controlled (Beaufort and Heussner, 2001). We have observed that progressive secondary calcification similarly affects these structures. The fact that, under the same diagenetic conditions, overgrowth is more evident on *E. huxleyi* than other coccoliths is probably related to the originally open disposition of the elements and to their crystallographic orientation. Most other species are constituted of directly butting elements, thus there is a smaller surface area for overgrowth to occur on and the effects are less obvious. Overgrowth will thicken elements but without greatly altering the SEM appearance, with LM this will result in brighter images but the distinction, during routine work, will be very subjective. Moreover, in *E. huxleyi* the distal shield elements have radial crystallographic *c*-axes which readily grow outwards, producing an irregular outline, whilst in many other taxa (e.g. *Calcidiscus leptoporus* or *Helicosphaera carteri*) the distal shield elements are oriented sub-vertically.

Carbonate dissolution in the water column and at the water/sediment interface has a stronger effect on the thin elements of *E. huxleyi* than on the more robust elements of other heterococcoliths (e.g. Dittert et al., 1999). Similarly, in the analysed sediments, the effects of carbonate dissolution are more visually detectable by SEM on *E. huxleyi* than on other coccoliths. Review of our SEM images lead us to conclude that *E. huxleyi* shows effects of carbonate dissolution/precipitation much more clearly than other coccoliths.

4.4. Emiliania huxleyi overgrowth index (EXO)—"Diagenetic" interval D1–D5

Given the sensitivity of *Emiliania huxleyi* to etching and overgrowth we developed an index of diagenesis based on relative abundance of the morphotypes:

$$\mathrm{EXO} = (\%\mathrm{EHMC}) + 2(\%\mathrm{ROC}) + (10(\%\mathrm{DY})/(\%\mathrm{EHLC}))$$

Coefficients have been used for ROC (2) and DY (10) in order to increase their significance since these forms are commonly lower in relative abundance than EHMC but are indicative of important carbonate precipitation in the environment.

This proxy has limitations related to the definition of EHLC that likely includes etched and OG1 forms. In particular, since EHLC is the dominant morphotype within sapropel S1 in all the Eastern Mediterranean cores (Figs. 3a–i), future studies are required to better evaluate effects of dissolution and/or overgrowth on coccoliths within this time interval.

In Figure 3, the EXO index is plotted. Characteristically, it shows similar patterns in most of the Eastern Mediterranean cores (Figs. 3a–i). To clarify discussion of these trends we identified 5 "Diagenetic" intervals indicated, from top to bottom, as D1 to D5. They are identified as follows (Figs. 3a–i and 4):

Diagenetic interval D5 is characterized by high values of EXO (usually close or greater than 10). Interruptions of this general trend are observed in tephra layers corresponding to sharp drops of EXO. The boundary with *Diagenetic interval D4* corre-

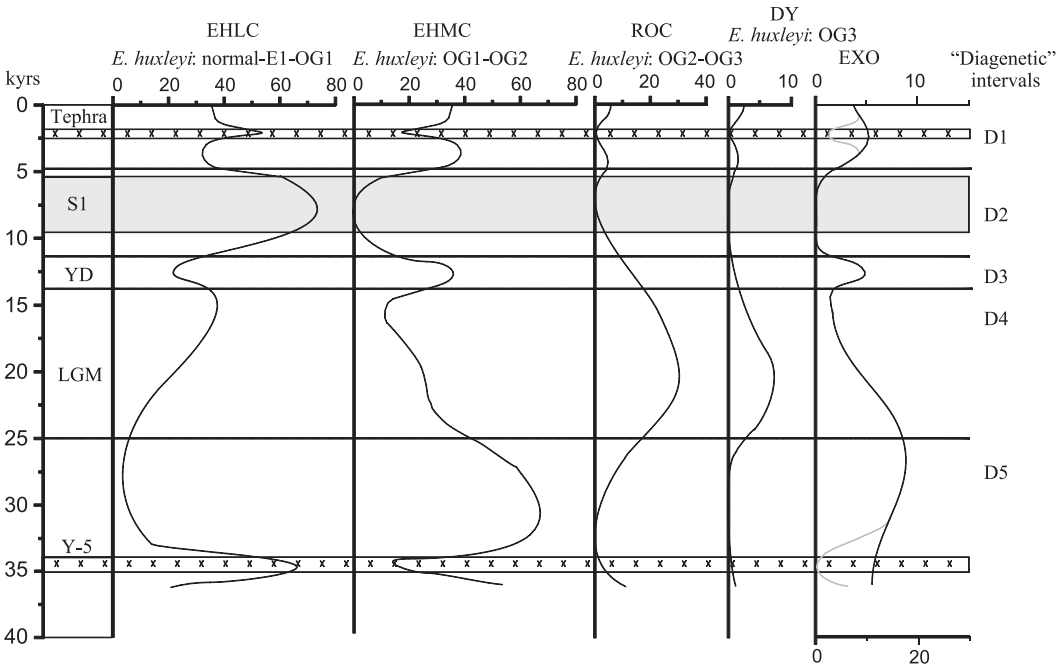

Fig. 4. Schematic figure representing the trend of *Emiliania huxleyi* LM-morphotypes (%) and EXO index in the studied stratigraphic interval. On the right side, the "Diagenetic" intervals D1–D5. Sapropel is traced on the base of estimated age of bottom of S1 and top of oxidised S1 calculated for low sedimentation rate cores by Mercone et al. (2000) (5.3 and 9.5 ka, respectively). A hypothetic Holocene tephra layer is also evidenced. Age of D1 lower limit is the mean of age of D1 obtained in the cores on the base of the sedimentation rate of S1 sapropel. The lower part of the figure has been constructed on the base of sedimentation rate of core BC3 calculated dating S1 bottom and tephta Y-5 (at 81.2 cm; 35 ka; Keller et al., 1978) as well as lower limits of D2–D4.

sponds to the end of the D5 plateau. In this interval a steady decrease of EXO is observed in all studied cores. *Diagenetic interval D3* is marked by a short-lived and small amplitude increase of EXO, falling to zero just before the base of sapropel S1. *Diagenetic interval D2* corresponds to sapropel S1, both the visual and the oxidized part and is characterized by values of EXO close to 0. Above sapropel S1, *Diagenetic interval D1* correlates with an increase of EXO, usually reaching values of approximately 5, but in tephras EXO shows major decreases.

4.5. Diagenetic history

4.5.1. Eastern Mediterranean

Variations in EXO index are time synchronous in the studied cores from the Eastern Mediterranean, despite their very different settings. Moreover, correlations with previous works (Violanti et al., 1991; Castradori, 1992, 1993b; Negri and Giunta, 2001; Principato et al., 2003) indicate that the identified diagenetic intervals can be traced through the basin. We therefore, speculate that D1 to 5 do not result from local diagenetic modifications, but reflect changes of bottom (and consequently interstitial) waters in the Eastern Mediterranean during the last 40 ka (Fig. 4).

The Last Glacial Maximum (LGM) corresponds to the end of the plateau in the EXO index, suggesting that diagenesis during the glacial interval mainly induced calcite precipitation on *Emiliania huxleyi* coccoliths and maximum overgrowth was reached in the time interval between the LGM and the Younger Dryas (YD).

The 2.5 ka long D3 broadly corresponds to the Younger Dryas (YD), where an increase of EXO indicates increase in carbonate precipitation on coccoliths.

The base of D2 shortly precedes the deposition of sapropel S1 and coincides with totally different

diagenetic modifications causing virtually no overgrowth of *E. huxleyi* coccoliths (EXO close to 0). SEM analyses of selected samples have qualitatively shown the more common presence of E1 coccoliths in the organic rich level than in the other intervals. This is further supported by our LM observation of thinner coccoliths in this interval (e.g. compare Plate I, figure 1 with figures 2–3). Moreover, within S1, we observed partial erosion and mechanical breakage of coccoliths (Plate II, figure 6) that together can be used as a proxy for coccolith dissolution (Ziveri et al., 1999a,b). The upper part of sapropel S1 has been subject to post-depositional downward oxidation that affected its original organic carbon and carbonate content (De Lange et al., 1989; Van Santvoort et al., 1996; Thomson et al., 1999; Mercone et al., 2000). However, the dark and oxidised portion of the sapropel is characterized by a similar abundance of the different LM morphotypes. This suggests that changes in the carbonate system are the main reason for the alteration of coccoliths, whereas other processes related to post depositional oxidation of the organic matter do not affect the coccoliths. The re-increase of EHMC at or just above the oxidised S1–S1 limit could indicate an early change in the carbonate diagenesis (i.e. initiation of more vigorous carbonate precipitation) before the end of anoxia.

In the past 5 ka, the EXO index reaches values similar to those of interval D4 (note the different scale of Fig. 3e and i.e. Fig. 3b). Noteworthy is its increase immediately after cessation of sapropel S1 formation that seems to correlate in all the Eastern Mediterranean cores. This could be an indication of an abrupt change in the carbonate-diagenetic processes that affected coccoliths.

4.6. Tephra-Emiliania huxleyi morphotypes

Some distinct peaks of EHLC over the other morphotypes are observed in association with tephra and/or FGF associated intervals (Figs. 3b–c,e; Table 5), suggesting that acidic interstitial waters induced preferential etching of *Emiliania huxleyi* coccoliths. However, there appears to be no systematic variation (e.g. Fig. 3a). Future studies are needed to clarify the relation between *E. huxleyi* diagenesis and the presence of amorphous silica or acidic volcanic components within the sediments.

4.7. Aegean Sea and Western Mediterranean

Despite the fact that it is not clear from our study if EHMC* is related to primary variation or to weak diagenesis, the index has also been applied to the cores from the Aegean Sea and Western Mediterranean and compared with results from the eastern basin (Fig. 3). In these cores the EXO index shows the lowest values (note the different scale adopted in plotting the EXO index in Figs. 3m–n) indicating much weaker overgrowth of coccoliths at these sites.

Further analyses are needed to completely characterise the primary or secondary variation of *Emiliania huxleyi* in these areas, but the available data strongly suggest that the distinctive diagenetic sequence seen in the Eastern Mediterranean is not developed elsewhere.

4.8. Atypical carbonate diagenesis

To our knowledge the type of abnormal early overgrowth of *Emiliania huxleyi* observed from these sediments (OG1–3) has not been reported in other pelagic sediments. Comparable diagenesis has, however, been reported in the Red Sea. Winter (1982a,b) recorded *E. huxleyi* coccoliths heavily affected by secondary calcite overgrowth and/or etching in late Quaternary sediments and discussed as the phenomena was likely an early diagenetic processes (Winter, 1982a). Winter (1982a) based on absence of dissolution of other carbonate shells reported by Reiss et al. (1980) also discussed that the observed dissolution effects on *E. huxleyi* were not related to dissolution in the water column. In the area altered *E. huxleyi* coccoliths (Winter, 1982a) appear to co-occurring with well-preserved holococcoliths as illustrated by Müller (1976). Small holococcoliths are prone to dissolution (Tappan, 1980), are selectively dissolved in the water column (Ziveri et al., 1999a, 2000b), commonly absent at the early stage of diagenesis in ancient sediments and very rare to absent in oceanic environment (e.g. Roth, 1974; Takahashi and Okada, 2000). These forms and other small heterococcoliths are more commonly found in shallow water areas (Müller et al., 1974; Müller, 1976; Winter, 1982b; Crudeli and Young, 2003).

Table 5
Semi-quantitative estimation of fine glass fragments (FGF) (LM, 1250 ×)
See text for symbol explanation. Grey colour: tephra presence as resulted from cores sedimentological description, LM observation of glass fragments (>150 and/or 63–150 μm fraction) and FGF. For simplification, intervals in which FGF are absent (N) are indicated by the depth of the lower and upper samples

MT15		UM42		AP01.1		SL114		SL73		BC3		ABC26		SL60		BC19		SL9		SL29	
Depth (cm)	FGF	Depth (cm)	FGF	Depth (cm)	FGF	Depth (cm)	FGF	Depth (cm)	FGF	Depth (cm)	FGF	Depth (cm)	FGF	Depth (cm)	FGF	Depth (cm)	FGF	Depth (cm)	FGF	Depth (cm)	FGF
1	N	0.7	N	0.5	N	0.5	S	0.9	N	14	N	0.4	N	1.5	N	0.5	N	0.7	S	0.5	S
3	S	6.15	N	1.5	N	4.5	S	5.4	N	74	N	10.6	N	4	N	2.5	N	1.7	N	1.5	N
5	N	6.9	S	2.5	S	5.5	N	6.4	S	75.2	S	11.2	S	6	S	3.5	S	6.7	N	9.5	N
7	N	7.65	C	3.5	N	6.8	N	7.4	S/C	76.4	C	11.8	S	8	S/C	4.5	N	7.7	S	10.5	S
9	S	8.65	N	4.5	S	7.8	A	18.9	S/C	77.6	S	12.4	S	10	S/C	7.75	N	8.7	S	11.5	S
13	S	34.65	N	5.5	N	8.8	A	19.9	S	79.4	S	13	N	12	S	9	S	9.7	N	12.5	N
15	N			8.5	N	9.8	N	20.9	C	81.2	C	26.2	N	20	S	9.75	A	10.7	N	22.5	N
17	S			9.5	S	10.8	S	33.5	C	82.4	S			22	S/C	10.5	A	11.7	S	23.5	S
19	C			10.5	N	11.8	N	34.5	S/C	83.6	S			30	S/C	11.5	S	15.7	S	24.5	N
21	N			12.5	N	12.8	S	35.5	S/C	84.8	N			32	S	12.5	N	16.7	N	39	N
23	S			13.5	S	17.8	S	36.5	C	86	N			34	A	34.7	N	17.7	S		
25	S			14.5	N	18.8	N	37.5	S					42	A			21.7	S		
27	N			16.7	N	19.8	S	38.5	S					44	VA			22.7	N		
29	N			18	S	20.8	N							56.5	VA			30.7	N		
31	S			19	N	21.8	N							59	N			31.7	S		
33	S			20	N	22.8	S							71	N			32.7	N		
35	N			21	S	24.8	S							73	S/C			44.2	N		
39	N			22.3	N	25.8	N							75	S/C						
41	C			23.5	S	32.3	N							77	N						
43	S			29.5	S	33.8	S							81	N						
45	N			30.5	N	34.8	N							83	S						
47	N			31.5	N	35.8	N							85	N						
49	S			32.7	N	36.8	S							87	S						
53	S			34	S	41.8	S							89	N						
55	N			35	S	42.8	N							91	S						
57	S			36	N	43.8	S							93	N						
59	N			40	N	46.9	S							95	S						
61	S			41	S	47.9	N							97	N						
63	N			48	S	48.9	N							162	N						
65	S			49	N									164	S						
67	S			50	N									170	S						
69	N			51.2	S									172	N						
71	S			53.5	S									176	N						
73	S			54.5	N									178.5	S						
75	N													184	S						
77	S													186	N						
79	S													188	N						
81	N													190	S						
83	N													192	N						
85	C													194	S						
87	N													196	N						
89	S													208	N						
91	N													210	S						
93	S																				
95	N																				
101	N																				
103	S																				
107	S																				
109	N																				
131	N																				
133	S																				
141	S																				

A particular feature of core-top sediments analysed in this work is the co-occurrence of well preserved holococcoliths, overgrown holococcoliths, small heterococcoliths and variably overgrown of *E. huxleyi* with also evidence of slight dissolution (Table 3; Plate I, figures 2–15; Plate II, figure 9; Crudeli and Young, 2003) and indicates complex processes related to carbonate dissolution and precipitation on coccoliths.

Coccoliths, including *E. huxleyi*, with incipient syntaxial overgrowth are common in Holocene–late Pleistocene hardgrounds widespread in the Eastern Mediterranean and less common in the western basin (Allouc, 1990; Aghib et al., 1991). Here, overgrowth appears to be related to precipitation of high-magnesian calcite from interstitial waters close to the sediment/water interface. Cita and Aghib (1991) illustrated an overgrown *Gephyrocapsa* specimen from an indurated level (incipient hardground) from a late Piacenzian condensed interval (Bannock Basin).

The Eastern Mediterranean sediments above and below sapropel S1 are characterised by inorganic–diagenetic precipitation of high-magnesium calcite, whereas S1 mainly contains other carbonate phases such as low-magnesium calcite and aragonite (Müller and Staesche, 1973; Milliman and Müller, 1973; Aksu et al., 1995b; Calvert and Fontugne, 2001; Thomson et al., in press).

It is possible that the diagenetic effects, visually detectable on *E. huxleyi*, are in some way related to the changes in the carbonate system that bring the sediments from high magnesium calcite dominated sediments outside the sapropel to other carbonate phase-dominated within the sapropel.

5. Conclusions

Quantitative studies of calcareous nannofossils in cores from the Eastern Mediterranean allowed the identification of coeval increases and decreases in abundance in the dominant *Emiliania huxleyi* as well as in other taxa. Detailed LM and SEM investigations revealed that various morphotypes of *E. huxleyi* and small bridgeless reticulofenestrids recorded from the Holocene–late Pleistocene of the Eastern Mediterranean represent different diagenetic stages of *E. huxleyi* coccoliths rather than a range of primary morphotypes or species. This clarification avoids spurious speculations on the paleoceanographic, biostratigraphic and microevolutionary significance of these morphotypes.

Based on our data and revision of previously published investigations, *E. huxleyi* seems a much more sensitive indicator of carbonate diagenesis than most other coccoliths. Detailed inspection of overgrowth and dissolution on *E. huxleyi* coccoliths is a powerful tool to trace the type and degree of diagenetic modifications. Even within a single sample a continuous variation from well-preserved *E. huxleyi* coccoliths to massively overgrown specimens with a complete sequence of intermediates between them have been observed. In the light of the SEM results, a correlation between LM morphotypes and subjectively defined overgrowth stages of forms has been proposed.

Based on the relative abundance of the LM-morphotypes and on their relation with overgrown coccoliths, the EXO index is proposed to identify Diagenetic Intervals (D1 to 5) and qualitatively trace the carbonate-diagenetic history of sediments in the Eastern Mediterranean during the past 40 ka.

A correspondence between diagenetic intervals D1 to 5 and major paleoceanographic episodes can be inferred based on high-resolution stratigraphy of the studied cores. During the last glacial interval bottom and interstitial waters lead to moderate recrystallization of *E. huxleyi* coccoliths and the strongest overgrowth occurred in the interval between the LGM and the YD. A drop of the EXO index shortly preceded the deposition of sapropel S1, when bottom and interstitial waters induced slight dissolution and no overgrowth of *E. huxleyi* coccoliths. Diagenetic modifications again caused overgrowth at the end of sapropel S1 deposition and persisted through the last 5 ka.

Our results indicate that (a) fluctuations in abundance of nannofossil morphotypes in the Eastern Mediterranean do not necessarily reflect environmental conditions in surface waters (temperature, fertility, etc.), but can be due to diagenetic overprint during (early) burial; (b) when morphotypes are the results of diagenesis, nannofossils can be used to trace the changes in the carbonate system; (c) different diagenetic processes affected coccoliths in the Western and eastern Mediterranean; (d) changes in diagenetic modifications are coeval within the eastern basin

and can, consequently, be used for local correlation within this basin.

The recognition of the abnormal diagenesis of *E. huxleyi* environment may provide valuable clues to diagenetic conditions in this area and possibly to the processes of sapropel formation.

Acknowledgements

This research has been predominantly funded by the EU. The initial quantitative LM study by DC was carried out as part of the SAP (MAS3-CT97-0137) project. The SEM study was carried out during a visit by DC to the NHM funded by *Sys-Resource* an Access to Research Infrastructures project of the EU-Improving Human Potential (IHP) Program. The research by JRY constitutes part of the CODENET TMR network project.

Chris Jones and Markus Geisen are thanked for assistance at the NHM. Agostino Rizzi and Saskia M. Kars assisted with previous SEM studies at the Dept. of Earth Sciences, Milano and Dept. of Earth Sciences, Amsterdam. DC thanks John Thomson and Llüisa Cros for informal advice on the improvement of the manuscript and M. Speranza Principato for data on presence of glass fragments. Furthermore, Luigina Vezzoli is warmly thanked for tephra analyses and Enno Schefuß for information on core UM42. We are grateful to Luc Beaufort and Mario Cachao for suggestions that helped improve the manuscript.

References

Aghib, F.S., Bernoulli, D., Weissert, H., 1991. Hardground formation in the Bannock Basin, Eastern Mediterranean. Mar. Geol. 100, 103–113.

Allouc, J., 1990. Quaternary crust on slopes of the Mediterranean Sea: A tentative explanation for their genesis. Mar. Geol. 94, 205–238.

Andruleit, H., 1996. A filtration technique for quantitative studies of coccoliths. Micropaleontology 42 (4), 403–406.

Aksu, A.E., Yasar, D., Mudie, P.J., 1995a. Paleoclimatic and paleoceanographic conditions leading to development of sapropel layer S1 in the Aegean Sea. Palaeogeogr. Palaeoclimatol. Palaeoecol. 116, 71–101.

Aksu, A.E., Yasar, D., Mudie, P.J., 1995b. Origin of late glacial-Holocene hemipelagic sediments in the Aegean Sea: clay mineralogy and carbonate cementation. Mar. Geol. 123, 33–59.

Aksu, A.E., Hiscott, R.N., Kaminski, M.A., Mudie, P.J., Gillespie, H., Abrajano, T., Yasar, D., 2002. Last glacial–Holocene paleoceanography of the Black Sea and Marmara Sea: stable isotopic, foraminiferal and coccolith evidence. Mar. Geol. 190, 119–149.

Beaufort, L., Heussner, S., 2001. Seasonal dynamics of calcareous nannoplankton on a West European continental margin: the Bay of Biscay. Mar. Micropaleontol. 43, 27–55.

Calvert, S.E., Fontugne, M.R., 2001. On the late Pleistocene–Holocene sapropel record of climatic and oceanographic variability in the eastern Mediterranean. Paleoceanography 16 (1), 78–94.

Castradori, D., 1992. I nannofossili calcarei come strumento per lo studio biostratigrafico e paleoceanografico del Quaternario nel Mediterraneo Orientale. PhD thesis, Univ. Milan, Italy.

Castradori, D., 1993a. Calcareous nannofossils and the origin of eastern Mediterranean sapropels. Paleoceanography 8 (4), 459–471.

Castradori, D., 1993b. Calcareous nannofossil biostratigraphy and biochronology in eastern Mediterranean deep-sea cores. Riv. Ital. Paleontol. Stratigr. 99 (1), 107–126.

Cita, M.B., Aghib, F.S., 1991. Evidence of relief inversion from the rim-syncline of Bannock Basin. Mar. Geol. 100, 67–81.

Colmenero-Hidalgo, E., Flores, J.-A., Sierro, F.J., 2002. Biometry of *Emiliania huxleyi* and its biostratigraphic significance in the Eastern North Atlantic Ocean and Western Mediterranean Sea in the last 20 000 years. Mar. Micropaleontol. 46 (3–4), 247–263.

Coltelli, M., Del Carlo, P., Vezzoli, L., 1998. Discovery of a Plinian basaltic eruption of Roman age at Etna volcano, Italy. Geology 26 (12), 1095–1098.

Corselli, C., Principato, M.S., Maffioli, P., Crudeli, D., 2002. Changes in planktonic assemblages during sapropel S5 deposition: evidence from Urania Basin area, eastern Mediterranean. Paleoceanography 17 (3) (10.1029/2000PA000536).

Cramp, A., O'Sullivan, G., 1999. Neogene sapropels in the Mediterranean: a review. Mar. Geol. 153, 11–28.

Cros, M.L., 2002. Planktonic coccolithophores of the NW Mediterranean. PhD thesis, Publicacions de la Universitat de Barcelona. Barcelona, Spain.

Crudeli, D., Young, J.R., 2003. SEM–LM study of holococcoliths preserved in Eastern Mediterranean sediments (Holocene/late Pleistocene). J. Nannoplankton Res. 25 (1), 39–50.

De Lange, G.J., Middelburg, J.J., Pruysers, P.A., 1989. Middle and Late Quaternary depositional sequences and cycles in the eastern Mediterranean. Sedimentology 36, 151–158.

De Lange, G.J., Van Santvoort, P.J.M., Langereis, C., Thomson, J., Corselli, C., Michard, A., Rossignol-Strick, M., Paterne, M., Anastasakis, G., 1999. Palaeo-environmental variations in Eastern Mediterranean sediments; a multidisciplinary approach in a prehistoric setting. Prog. Oceanogr. 44, 369–386.

Dittert, N., Baumann, K.-H., Bickert, T., Henrich, R., Huber, R., Kinkel, H., Meggers, H., 1999. Carbonate dissolution in the Deep-Sea: Methods, Quantification and Paleoceanographic Application. In: Fischer, G., Wefer, G. (Eds.), Use of Proxies in Paleoceanography: Examples from the South Atlantic. Springer-Verlag, Berlin, Heidelberg, pp. 255–284.

Flores, J.-A., Sierro, F.J., Francés, G., Vázquez, A., Zamarreño, I.,

1997. The last 100,000 years in the western Mediterranean: sea surface water and frontal dynamics as revealed by coccolithophores. Mar. Micropaleontol. 29, 351–366.

Flores, J.-A., Gersonde, R., Sierro, F.J., 1999. Pleistocene fluctuations in the Agulhas Current Retroflection based on the calcareous plankton record. Mar. Micropaleontol. 37, 1–22.

Freydier, R., Michard, A., De Lange, G.J., Thomson, J., 2001. Nd isotopic composition of Eastern Mediterranean sediments: traces of the Nile influence during sapropel S1 formation? Mar. Geol. 177, 45–62.

Gartner, S., 1977. Calcareous nannofossil biostratigraphy and revised zonation of the Pleistocene. Mar. Micropaleontol. 2, 1–25.

Giunta, S., Negri, A., Morigi, C., Capotondi, L., Combourieu-Nebout, N., Emeis, K.C., Sangiorgi, F., Vigliotti, L., 2003. Coccolithophorid ecostratigraphy and multi-proxy paleoceanographic reconstruction in the Southern Adriatic Sea during the last deglacial time (Core AD91-17). Palaeogeogr. Palaeoclimatol. Palaeoecol. 190, 39–59.

Henriksson, A.S., 2000. Coccolithophores response to oceanographic changes in the equatorial Atlantic during the last 200,000 years. Palaeogeogr. Palaeoclimatol. Palaeoecol. 156, 161–173.

Hilgen, F.J., 1991. Astronomical calibration of Gauss to Matuyama sapropels in the Mediterranean and implication for the geomagnetic polarity time scale. Earth Planet. Sci. Lett. 104, 226–244.

Jordan, R.W., Kleijne, A., 1994. A classification system for living coccolithophores. In: Winter, A., Siesser, W.G. (Eds.), Coccolithophores. Cambridge University Press, Cambridge, pp. 83–105.

Keller, J., Ryan, W.B.F., Ninkovich, D., Altherr, R., 1978. Explosive volcanic activity in the Mediterranean over the past 200,000 yr as recorded in deep-sea sediments. Geol. Soc. Amer. Bull. 89, 591–604.

Kinkel, H., Baumann, K.-H., Cepek, M., 2000. Coccolithophores in the equatorial Atlantic Ocean: response to seasonal and Late Quaternary surface water variability. Mar. Micropaleontol. 39, 87–112.

Kleijne, A., 1993. Noelaerhabdaceae, Syracosphaeraceae and other species. Morphology, taxonomy and distribution of extant coccolithophorids (Calcareous nannoplankton), Published PhD thesis, Vrije Universitaeit, Amsterdam, Drukkerij FEBO, Enschede. Katwijk. The Netherlands, pp. 227–262.

Knappertsbusch, M., 1993. Geographic distribution of living and Holocene coccolithophores in the Mediterranean Sea. Mar. Micropaleontol. 21, 219–247.

Lourens, L.J., Antonarakou, A., Hilgen, F.J., Van Hoof, A.A.M., Vergnaud-Grazzini, C., Zachariasse, W.J., 1996. Evaluation of the Plio-Pleistocene astronomical timescale. Paleoceanography 11, 391–413.

Matsuoka, H., Okada, H., 1989. Quantitative Analysis of Quaternary Nannoplankton in the Subtropical Northwestern Pacific Ocean. Mar. Micropaleontol. 14, 97–118.

McIntyre, A., 1969. The coccolithophorida in Red Sea sediments. In: Degens, E.T., Ross, D.A. (Eds.), Hot Brines and Recent Heavy Metal Deposits in the Red Sea. Springer-Verlag, New York, pp. 299–305.

Mercone, D., Thomson, J., Croudace, I.W., Siani, G., Paterne, M., Troelstra, T., 2000. Duration of S1, the most recent sapropel in the eastern Mediterranean Sea, as indicated by AMS radiocarbon and geochemical evidence. Paleoceanography 15, 336–347.

Milliman, J.D., Müller, J., 1973. Precipitation and lithification of magnesian calcite in the deep-sea sediments of the eastern Mediterranean Sea. Sedimentology 20, 29–45.

Müller, C., 1976. Nannoplankton-Gemeinschaften aus dem Jung-Quartär des Golfes von Aden and des Rotes Meeres. Geol. Jahrb., Beih. D17, 33–77.

Müller, J., Staesche, W., 1973. Precipitation and diagenesis of carbonates in the Ionian deep-sea. Bull. Geol. Soc. Greece 10 (1), 145–151.

Müller, C., Blanc Vernet, L., Chamley, H., Froget, C., 1974. (1975) Les Coccolithophorides d'une carotte Méditerranéenne, Comparaison Paléoclimatologique avec les foraminifères, les Ptéropodes et les argiles. Tethys 6 (4), 805–827.

Narcisi, B., Vezzoli, L., 1999. Quaternary stratigraphy of distal tephra layers in the Mediterranean—an overview. Glob. Planet. Change 21, 31–50.

Negri, A., Giunta, S., 2001. Calcareous nannofossil paleoecology in the sapropel S1 of the eastern Ionian sea: paleoceanographic implications. Palaeogeogr. Palaeoclimatol. Palaeoecol. 169, 101–112.

Negri, A., Villa, G., 2000. Calcareous nannofossil biostratigraphy, biochronology and paleoecology at the Tortonian/Messinian boundary of the Faneromeni section (Crete). Palaeogeogr. Palaeoclimatol. Palaeoecol. 156, 195–209.

Negri, A., Capotondi, L., Keller, J., 1999a. Calcareous nannofossils, planktonic foraminifera and oxygen isotopes in the late Quaternary sapropels of the Ionian Sea. Mar. Geol. 157, 89–103.

Negri, A., Giunta, S., Hilgen, F.J., Krijgsman, W., Vai, G.B., 1999b. Calcareous nannofossil biostratigraphy of the M. del Casino section (northern Apennines, Italy) and paleoceanographic conditions at times of Late Miocene sapropel formation. Mar. Micropaleontol. 36, 13–30.

Okada, H., McIntyre, A., 1977. Modern coccolithophores of the Pacific and North Atlantic oceans. Mar. Micropaleontol. 23 (1), 1–55.

Okada, H., Wells, P., 1997. Late Quaternary nannofossil indicators of climate change in two deep-sea cores associated with the Leeuwin Current off Western Australia. Palaeogeogr. Palaeoclimatol. Palaeoecol. 131, 413–432.

Principato, M.S., 2003. Late Pleistocene–Holocene planktonic foraminifera from the eastern Mediterranean Sea: towards a high-resolution planktonic foraminiferal assemblage zonation for the Late Quaternary of the Mediterranean. Riv. Ital. Paleontol. Stratigr. 109 (1), 111–124.

Principato, M.S., Giunta, S., Corselli, C., Negri, A., 2003. Late Pleistocene–Holocene planktonic assemblages in three box-cores from the Mediterranean Ridge area (west–southwest of Crete): palaeoecological and palaeoceanographic reconstruction of sapropel S1 interval. Palaeogeogr. Palaeoclimatol. Palaeoecol. 190, 61–77.

Raffi, I., Flores, J.-A., 1995. Pleistocene through Miocene calcareous nannofossils from eastern equatorial Pacific Ocean (Leg 138). In: Pisias, N.G., Mayer, L.A., Janecek, T.R., Palmer-Julson, A., van Andel, T.H. (Eds.), Proc. ODP, Sci. Results, vol. 138, pp. 233–286.

Raffi, I., Backman, J., Rio, D., Shackleton, N.J., 1993. Plio-Pleistocene nannofossil biostratigraphy and calibration to Oxygen Isotope stratigraphies from Deep Sea Drilling Project Site 607 and Ocean Drilling Program Site 677. Paleoceanography 8, 387–408.

Rahman, A., de Vernal, A., 1994. Surface oceanographic changes in the eastern Labrador Sea: Nannofossil record of the last 31,000 years. Mar. Geol. 121, 247–263.

Ramsay, A.T.S., 1972. Aspects of the distribution of fossil species of calcareous nannoplankton in North Atlantic and Caribbean sediments. Nature 236, 67–70.

Rio, D., Raffi, I., Villa, G., 1990. Pliocene–Pleistocene calcareous nannofossil distribution patterns in the western Mediterranean. In: Kastens, K.A., Mascale, J., et al. (Eds.), Proc. ODP, Sci. Results, vol. 107, pp. 513–533.

Reiss, Z., Luz, B., Almogi-Labin, A., Halicz, E., Winter, A., Wolf, M., 1980. Late Quaternary Paleoceanography of the Gulf of Aqaba (Elat), Red Sea. Quat. Res. 14, 294–308.

Rossignol-Strick, M., 1985. Mediterranean Quaternary sapropels, an immediate response of the African monsoon to variation of insolation. Paleogeogr. Palaeoclimatol. Palaeoecol. 49, 237–263.

Rossignol-Strick, M., Nesteroff, W., Olive, P., Vergnaud-Grazzini, C., 1982. After the deluge: Mediterranean stagnation and sapropel formation. Nature 295, 105–110.

Roth, P.H., 1973. Calcareous nannofossils—Leg 17. Init. Repts. DSDP 17, 695–795.

Roth, P.H., 1974. Calcareous nannofossils from the northwestern Indian Ocean, Leg 24, Deep Sea Drilling Project. Init. Repts. DSDP 24, 969–994.

Roth, P.H., 1978. Cretaceous nannoplankton biostratigraphy and oceanography of the northwestern Atlantic Ocean. Init. Repts. DSDP 44, 731–759.

Roth, P.H., 1983. Jurassic and Lower Cretaceous calcareous nannofossils in the western north Atlantic (Site 534): biostratigraphy, preservation, and some observations on biogeography and paleoceanography. Init. Repts. DSDP 76, 587–621.

Roth, P.H., Thierstein, H., 1972. Calcareous nannoplankton: leg 14 of the Deep Sea Drilling Program. Init. Repts. DSDP 14, 421–485.

Sbaffi, L., Wezel, F.C., Kallel, N., Paterne, M., Cacho, I., Ziveri, P., Shackleton, N., 2001. Response of the pelagic environment to palaeoclimatic changes in the central Mediterranean Sea during the Late Quaternary. Mar. Geol. 178, 39–62.

Su, X., Baumann, K.-H., Thiede, J., 2000. Calcareous nannofossils from Leg 168: biochronology and diagenesis. In: Fisher, A., Davis, E.E., Escutia, C. (Eds.), Proc. ODP, Sci. Results, vol. 168, pp. 39–49.

Takahashi, K., Okada, H., 2000. The paleoceanography for the last 30,000 years in the southeastern Indian Ocean by means of calcareous nannofossils. Mar. Micropaleontol. 40, 83–103.

Tappan, H., 1980. Haptophyta, coccolithophores, and other calcareous nannoplankton. The Paleobiology of Plant Protists. W.H. Freeman and Company, San Francisco, CA, pp. 678–803.

Thierstein, H.R., 1980. Selective dissolution of Late Cretaceous and Early Tertiary Calcareous nannofossils: experimental evidence. Cretac. Res. 2, 165–176.

Thierstein, H.R., Geitzenauer, K.R., Molfino, B., Shackleton, N.J., 1977. Global synchroneity of late Quaternary coccolith datum levels: validation by oxygen isotopes. Geology 5, 400–404.

Thomson, J., Crudeli, D., de Lange, G.J., Slomp, C.P., Erba, E., Corselli, C. and Calvert, S.E., in press. *Florisphaera profunda* and the origin and diagenesis of carbonate phases in eastern Mediterranean sapropel units. Paleoceanography.

Thomson, J., Mercone, D., de Lange, G.J., van Santvoort, P.J.M., 1999. Review of recent advances in the interpretation of eastern Mediterranean sapropel S1 from geochemical evidence. Mar. Geol. 153, 77–89.

Van Santvoort, P.J.M., de Lange, G.J., Thomson, J., Cussen, H., Wilson, T.R.S., Krom, M.D., Ströhle, K., 1996. Active post-depositional oxidation of the most recent sapropel (S1) in sediments of the eastern Mediterranean Sea. Geochim. Cosmochim. Acta 60 (21), 4007–4024.

Violanti, D., Grecchi, G., Castradori, D., 1991. Paleoenvironmental interpretation of core Ban 88-11GC (Eastern Mediterranean, Pleistocene–Holocene-) on the grounds of Foraminifera, Thecosomata and calcareous nannofossils. Il Quaternario 4 (1a), 13–39.

Wells, P., Okada, H., 1997. Response of nannoplankton to major changes in sea-surface temperature and movements of hydrological fronts over Site DSDP 594 (south Chatham Rise, southeastern New Zealand), during the last 130 kyr. Mar. Micropaleontol. 32, 341–363.

Winter, A., 1982a. Post-depositional shape modification in Red Sea coccoliths. Micropaleontology 28 (3), 319–323.

Winter, A., 1982b. Paleoenvironmental interpretation of Quaternary coccolith assemblages from the Gulf of Aqaba (Elat), Red Sea. Rev. Esp. Micropaleontol. 14, 291–314.

Young, J.R., 1989. Observations on heterococcolith rim structure and its relationship to developmental processes. In: Crux, J., van Heck, S.E. (Eds.), Nannofossils and their Biostratigraphic Applications. Ellis Horwood, Chichester, pp. 1–20.

Young, J.R., 1990. Size variation of Neogene *Reticulofenestra* coccoliths from Indian Ocean DSDP cores. J. Micropaleontol. 9, 71–85.

Young, J.R., 1994. Variation in *Emiliania huxleyi* coccolith morphology in samples from the Norwegian EHUX experiment. Sarsia 79, 417–425.

Young, J.R., 1998. Neogene nannofossils. In: Bown, P.R. (Ed.), Calcareous Nannofossil Biostratigraphy. British Micropalaeontology Society Series, pp. 225–265.

Young, J.R., Westbroek, P., 1991. Genotypic variation in the coccolithophorid species *Emiliania huxleyi*. Mar. Micropaleontol. 18, 5–23.

Young, J.R., Kucera, M., Chung, H.-W., 1996. Automated biometrics on captured light microscope images of coccolith of *E. huxleyi*. In: Moguilevsky, A., Whatley, R., (Eds.), Microfossils and Oceanic Environments. Univ. of Wales, Aberystwyth Press, pp. 261–280.

Young, J.R., Bergen, J.A., Bown, P.R., Burnett, J.A., Fiorentino, A., Jordan, R.W., Kleijne, A., van Niel, B.E., Romein, A.J.T., von Salis, K., 1997. Guidelines for coccolith and calcareous nannofossil terminology. Palaeontology 40, 875–912.

Ziveri, P., Young, J.R., van Hinte, J.E., 1999a. Coccolithophore Export Production and Accumulation Rates. On Determination

of Sediment Accumulation Rates. GeoResearch Forum, vol. 5. Trans Tech Publications, Switzerland, pp. 41–56.

Ziveri, P., Ganssen, G.M., van Hinte, J.E., Young, J.R., 1999b. Quantification of calcium carbonate dissolution in the northeast Atlantic. European Union of Geosciences, EUG10, 28th March–1st April, Strasbourg. Abstract, vol. 247.

Ziveri, P., Rutten, A., De Lange, G.J., Thomson, J., Corselli, C., 2000a. Present-day coccolith fluxes recorded in central eastern Mediterranean sediment traps and surface sediments. Palaeogeogr. Palaeoclimatol. Palaeoecol. 158, 175–195.

Ziveri, P., Broerse, A.T.C., van Hinte, J.E., Westbroek, P., Honjo, S., 2000b. The fate of coccoliths at 48°N 21°W, northeastern Atlantic. Deep-Sea Res. II 47, 1853–1875.